Electronic Supplementary Material (ESI) for Physical Chemistry Chemical Physics.


# Structural Relaxation, Viscosity, and Network Connectivity in a Hydrogen Bonding Liquid.

Stefania Perticaroli[a,b,†,*], Barmak Mostofian[c,d,e,†], Georg Ehlers[f], Joerg C. Neuefeind[g], Souleymane O. Diallo[g], Christopher B. Stanley[b], Luke Daemen[g], Takeshi Egami[a,h], John Katsaras[a,b,h], Xiaolin Cheng[c,e,i], Jonathan D. Nickels[a,b,h,†,*]

[a] *Shull Wollan Center, a Joint Institute for Neutron Sciences, Oak Ridge National Laboratory, Oak Ridge, TN, 37831, USA.*
[b] *Biology and Soft Matter Division, Oak Ridge National Laboratory, Oak Ridge, TN, 37831, USA.*
[c] *Center for Molecular Biophysics, Oak Ridge National Laboratory, Oak Ridge, TN, 37831, USA.*
[d] *Joint Institute for Biological Sciences, Oak Ridge National Laboratory, Oak Ridge, TN, 37831, USA.*
[e] *BioEnergy Science Center, Oak Ridge National Laboratory, Oak Ridge, TN, 37831, USA.*
[f] *Quantum Condensed Matter Division, Oak Ridge National Laboratory, Oak Ridge, TN, 37831, USA.*
[g] *Chemical and Engineering Materials Division, Oak Ridge National Laboratory, Oak Ridge, TN, 37831, USA*
[H] *Department of Physics and Astronomy, University of Tennessee, Knoxville, TN, 37996.*
[I] Department of Biochemistry & Cellular and Molecular Biology, *University of Tennessee, Knoxville, TN, 37996.*
† These authors contributed equally.
*Corresponding authors.

## Electronic Supporting Information

This document contains:

Materials and Methods, 6 Supporting Figure, 1 Supporting Table

Two Supporting Movie Files can be found at:

Nanosecond/Picosecond Dynamics of NMA - Full Molecule

https://youtu.be/MQR_63ZcP5Q

and

Nanosecond/Picosecond Dynamics of NMA - H-bond Network

https://youtu.be/9hCI3E4dKXY

## Materials and Methods

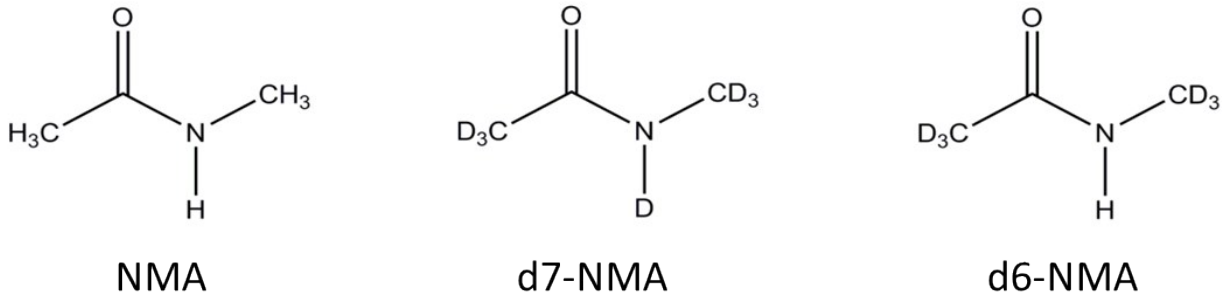


**Figure S1.** Structure of n-methylacetamide (NMA) and deuteration schemes used in this work.

### Samples

d7-NMA and NMA were purchased from Sigma-Aldrich, d6-NMA was purchased from CDN isotopes. Molecular formulas are reported in Figure S1; calculated incoherent and coherent scattering contributions for each sample in Table S1.

**Table S1** Incoherent and coherent scattering contributions for each studied sample. This calculation is based on the molecular formulas and sample masses, the NIST database was used to obtain the scattering cross sections (https://www.ncnr.nist.gov/resources/n-lengths/).

| Scattering contribution | Incoherent | Coherent |
|---|---|---|
| NMA | 92.7% | 7.3% |
| d6-NMA | 58.1% | 41.9% |
| d7-NMA | 17.3% | 82.7% |

### Neutron diffraction

Neutron diffraction measurements were conducted at the Nanoscale Ordered Materials Diffractometer (NOMAD) at the Oak Ridge National Laboratory (ORNL) Spallation Neutron Source (SNS), Oak Ridge, Tennessee, U.S.A. [1]. Standard instrument settings at 60 Hz have been used to access the q range of 0.2-50 $Å^{-1}$. Samples were sealed in 5 mm diameter Wilmad NMR tubes and measured for 2 hours at 303K. S(q) was obtained by normalizing diffraction data against a solid vanadium rod and subtracting the background using the IDL routines developed for the NOMAD instrument. Perdeuterated NMA (d7-NMA) was used because substituting deuterium for hydrogen presents us with two distinct advantages for scattering studies, a lower incoherent scattering background, in addition to the larger coherent scattering contribution for deuterium-deuterium correlations.

### Neutron scattering spectroscopy

Quasielastic and inelastic neutron scattering experiments were performed at ORNL at SNS, on two instruments: the Backscattering Spectrometer (BASIS)[2] and at the time-of-flight Cold Neutron Chopper Spectrometer (CNCS)[3]. Elastic resolutions were 3.5 μeV (~300 ps) on BASIS and ~50 μeV (~20 ps) on CNCS; giving access to q ranges of 0.2−2 and 0.2−4 $Å^{-1}$, respectively. This combination of spectrometers

covers over more than three orders in energy (from ~3.5 μeV up to ~20 meV) allowing the investigation of dynamics from hundreds of picoseconds to femtoseconds. Neutron experiments were carried out at 303K. Closed cycle refrigerator was used to control the sample temperature at BASIS; a standard 'Orange' cryostat was employed at CNCS. In both sets of experiments the cans were placed in helium exchange gas atmosphere to ensure homogeneous temperature. Samples were placed in standard annular aluminum sample cans used at the BASIS and CNCS instruments, using inner spacers with a 0.1 mm gap for NMA and 2 mm gap for d7-NMA, and closed including an indium seal. All the spectra were corrected for the sample can and normalized to the scattering from vanadium. No multiple scattering corrections were used. Data reduction for BASIS and CNCS spectra was performed using the Mantid software environment[4].

The formalism chosen to display neutron spectra in the full frequency ranges is the imaginary part of the dynamic susceptibility, $\chi''(q,\nu)$. Spectra from CNCS were experimentally obtained on the energy gain side and experiments at BASIS used the energy loss side of the spectra. In the energy gain side, the neutron scattering dynamic susceptibility was calculated as:

$$\chi''(q,\nu) \propto \frac{S(q,\nu)}{n_B(\nu)} \qquad \textit{(S1)}$$

where S(q,ν) is the measured dynamic structure factor and $n_B(\nu) = [exp(h\nu/kT) - 1]^{-1}$ is the Bose occupation number [5].

In the case of the energy loss side of the spectra, the susceptibility is calculated according to equation:

$$\chi''(q,\nu) \propto \frac{S(q,\nu)}{n_B(\nu) + 1} \qquad \textit{(S2).}$$

This representation is particularly convenient to visualize relaxation dynamics since trivial temperature effects are taken into account and well-separated relaxation processes appear as separate peaks. The position of the maximum of the peak provides an estimate of the characteristic relaxation time, and its spectral shape gives information about the stretching of the process.

The NS spectra can be modeled as the sum of several empirical relaxation functions which have found widespread acceptance in describing the molecular relaxations observed in the frequency domain[6, 7]. A Cole-Davidson function (CD);

$$\chi''_{CD}(\nu) = -Im\left\{\Delta_{CD}\left[1 + i2\pi\nu\tau_{CD}\right]^{-\beta_{CD}}\right\} \qquad \text{(S3)},$$

was used to account for the self-diffusion of NMA, a Cole-Cole function (CC);

$$\chi''_{CC}(\nu) = -Im\left\{\Delta_{CC}\left[1 + \left(i2\pi\nu\tau_{CC}\right)^{\alpha}\right]^{-1}\right\} \qquad \text{(S4)},$$

was used to account for the rattling in a cage process around 1-2 ps, and two Brownian oscillators were used to account for the librational motions (Figure 4a). From this approach, we obtained the amplitude, Δ, and relaxation time, τ , of the processes; as well as the stretching exponents which reflects the non-Gaussian character of the underlying dynamical process. These exponents were roughly constant for q-values, averaging at $\beta_{CD}^{diff} = 0.73$ and $\alpha_{CC}^{rattl} = 0.83$. Moreover, the spectra of NMA are dominated by a clear peak at low energy that shifts strongly to higher energy with increase in q (Figure 5c). This feature is associated with single-molecule and has been observed with Kerr-effect spectroscopy experiments[8].

With NS, we have access to the q-dependence of the diffusional component, $\tau_{CD}^{diff}$, allowing us to use a

stretched jump diffusion model to extact the self-diffusion coefficient. This model is used because of the the non-Gaussian character of the underlying dynamical process, through the relation:

$$\tau_{CD}^{diff} = \tau_0\left[1 + \frac{1}{q^2 l_0^2}\right]^{\frac{1}{\beta_{CD}^{diff}}} \quad \text{(S5)},$$

where $l_0$ represents the jump distance, $\tau_0$ the residence time (jump time) and $\beta_{CD}^{diff}$ is the stretching parameter describing the shape of the relaxation function[9] (Figure 4b). This model yields $l_0$=(1.70±0.02) Å as a jump distance, $\tau_0$ =(19.1±0.3) ps as a residence time, and gives an estimate of the effective self-diffusion coefficient at 0.44±0.05x10$^{-5}$ cm$^2$/s (Figure S4), in good agreement NMR experiments and MD simulations[10, 11]. Average relaxation times, $\langle\tau\rangle$, are reported to reflect the mean relaxation time from the underlying distribution rather than that of the experimental fit and was calculated as, $\langle\tau_{CD}\rangle = \tau_{CD}\beta_{CD}$, where $\tau_{CD}$ and $\beta_{CD}$ the parameters of the fit.

Additional inelastic neutron scattering (INS) measurements were performed on the Vibrational Spectrometer (VISION) at ORNL at SNS.[12] Each sample (∼1 g) was loaded into 8 mm diameter vanadium cylindrical canisters sealed with copper gaskets and then cooled to the base temperature. Measurement of an empty V-canister of the same type was used for background subtraction. Experiments were carried out at 10K. Data is presented in the intensity formalism.

**MD simulations**

All-atom MD simulations of liquid NMA were performed on a set of 27,000 NMA molecules randomly placed in a cubic box. After energy-minimization, the system was equilibrated for 40 ns with the box lengths converging to ~15 nm. The system size was chosen such that the potential formation of relatively long NMA chains (at least 10 molecules) would not be impacted by boundary effects. Simulations were conducted in the NPT ensemble at 310 K, which corresponds to $T_M$ + 5 K, to mirror the experimental measurements.. Non-bonding interactions were cut off at 12 Å and long-range electrostatic interactions were treated using the particle-mesh Ewald (PME) method with a 1 Å grid spacing.[13] Bonds to hydrogens were constrained using the LINCS algorithm[14] and 2 fs time steps were used. For the structural characterization, the simulation was performed for over 250 ns and the coordinates were saved at 1 ps intervals for evaluation. For the analysis of dynamics, the simulation was restarted for 5 ns with a 10 fs time resolution. All simulations were performed using the Charmm force field[15] and the Gromacs software suite[16] on the Oak Ridge Leadership Computing Facility (OLCF).

The translational mean square displacement was evaluated as;

$$\langle r^2(t)\rangle = \frac{1}{N}\sum_i \left|\vec{r}_i(t) - \vec{r}_i(0)\right|^2 \quad \text{(S6)},$$

with $\vec{r}_i(t)$ and $\vec{r}_i(0)$ representing the positions of the center of mass of molecule *i* at times t and 0, respectively[17]. The rotational mean square displacement was obtained for the vector rotational displacement[17, 18], $\vec{\varphi}_i(\Delta t)$;

$$\langle \varphi^2(t) \rangle = \frac{1}{N} \sum_i \left| \vec{\varphi}_i(t) - \vec{\varphi}_i(0) \right|^2 \quad \text{(S7)},$$

along two different axes of the NMA molecule, the $\vec{CN}$ and $\vec{CO}$ vectors.

The non-Gaussian parameter, α(t), describes the deviation from a Gaussian distribution of the self-part of the van Hove correlation function $G_s(r,t)$ [19] and allows us to detect the presence of dynamical heterogeneities in both the translational, $\alpha_{TRANSL}(t)$[20], and rotational $\alpha_{ROT}(t)$[17, 18], motions. We calculate the parameter for both the translational motions, $\alpha_{TRANSL}(t)$[20], and rotational motions, $\alpha_{ROT}(t)$[17, 18] as:

$$\alpha_{TRANSL}(t) = 3\langle r^4(t) \rangle / 5\langle r^2(t) \rangle^2 - 1 \quad \text{(S8)},$$

and,

$$\alpha_{ROT}(t) = 3\langle \varphi^2(t) \rangle / 5\langle \varphi^2(t) \rangle^2 - 1 \quad \text{(S9)}.$$

The mean first passage time (MFPT) for newly formed HBs[21-23] was calculated considering a forward rate constant $\frac{1}{k} = \langle \tau_{HB}^{MFPT} \rangle$. This is accomplished by computing a histogram of HB lifetimes, $P_{HB}(t)$, which can be related to a survival probability for the newly formed HB (Figure 6a) and $\langle \tau_{HB}^{MFPT} \rangle$ through the series of relations:

$$\langle \tau_{HB}^{MFPT} \rangle = \int_0^\infty s_{HB\ break}(t)dt = \int_0^\infty tP_{HB}(t)dt \quad \text{(S10)}.$$

Alternately, it is often more convenient, however, to treat the corresponding autocorrelation function, $c(t)$, which can be fit with multiple decay functions. Here we use the Kohlrausch-Williams-Watts function[24, 25] (WW), which takes the form of a stretched exponential decay, $e^{-\left(t/\tau_{WW}\right)^{\beta_{WW}}}$. This has the advantage of better describing the shape of non-Gaussian distributions and resolving multiple components when more than one process controls a given molecular event. As with the experimental results, we report the average lifetime/relaxation time for stretched processes, which can be calculated as $\langle \tau_{WW} \rangle = \frac{\tau_{WW}}{\beta_{WW}} \Gamma\left[\frac{1}{\beta_{WW}}\right]$, where $\tau_{ww}$ and $\beta_{ww}$ are the fit parameters and Γ is the gamma function[6].

We estimated the free energy of activation, $\Delta G^{\ddagger}$, for the breaking of H-bonds using the time scale of H-bond breaking. Assuming the process to follow the Eyring model[26], we applied the formula;

$$\langle \tau_{HB} \rangle = \frac{h}{k_B T} exp\left(\frac{\Delta G^{\ddagger}}{k_B T}\right) \quad \text{(S11)},$$

yielding a value of $\Delta G^{\ddagger}$=5.9 kJ/mol. We also computed the free energy of the formation of a H-bond at $T_m$+5K using the formula:

$$\Delta G = k_B T ln\left(\frac{N_{HB}}{N_{max} - N_{HB}}\right) \quad \text{(S12)},$$

where our simulation box contained 27,000 potential H-bonds, $N_{max}$, and the average number of H-

bonds, $N_{HB}$, was 21,967±42, $k_B$ is the Boltzmann constant, T is the temperature (310K); yielding an estimate of the free energy of hydrogen bonding at 3.8±0.2 kJ/mol.

**Supplementary Figures**

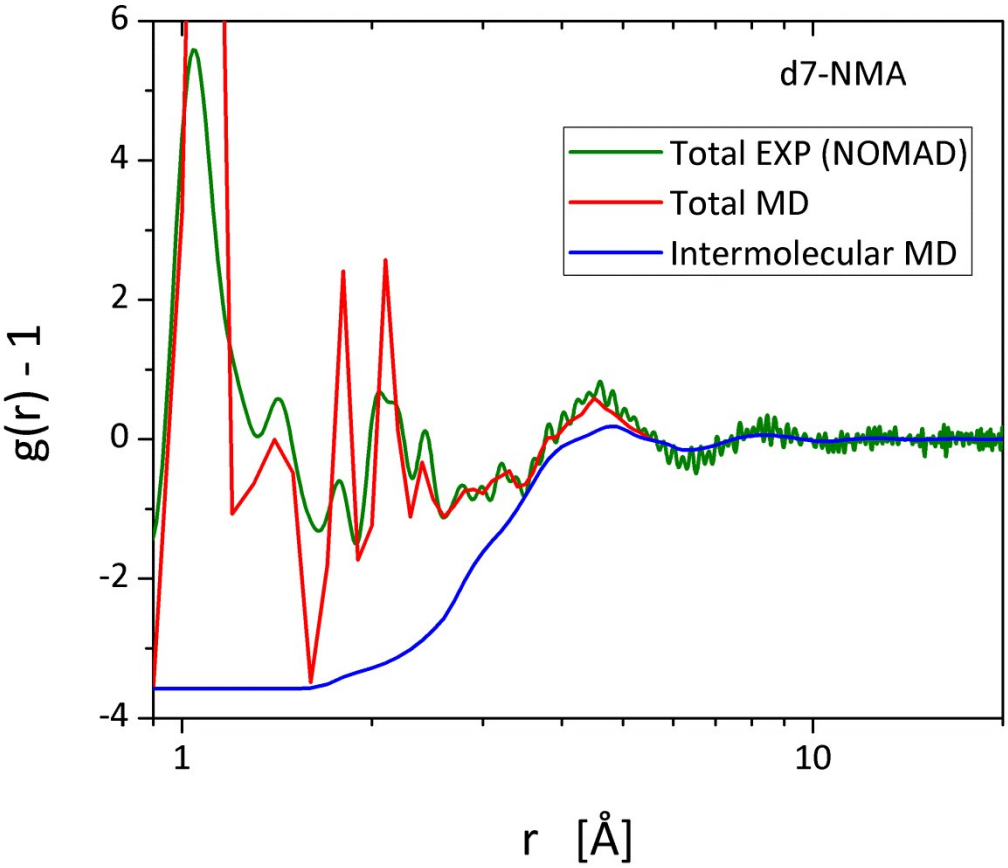


**Figure S2** The radial distribution function g(r) computed from MD and its comparison to g(r) computed from experimental data collected on the NOMAD spectrometer. Note the intermolecular contribution superimposed in analogy to the inset of Figure 1a of the main text.

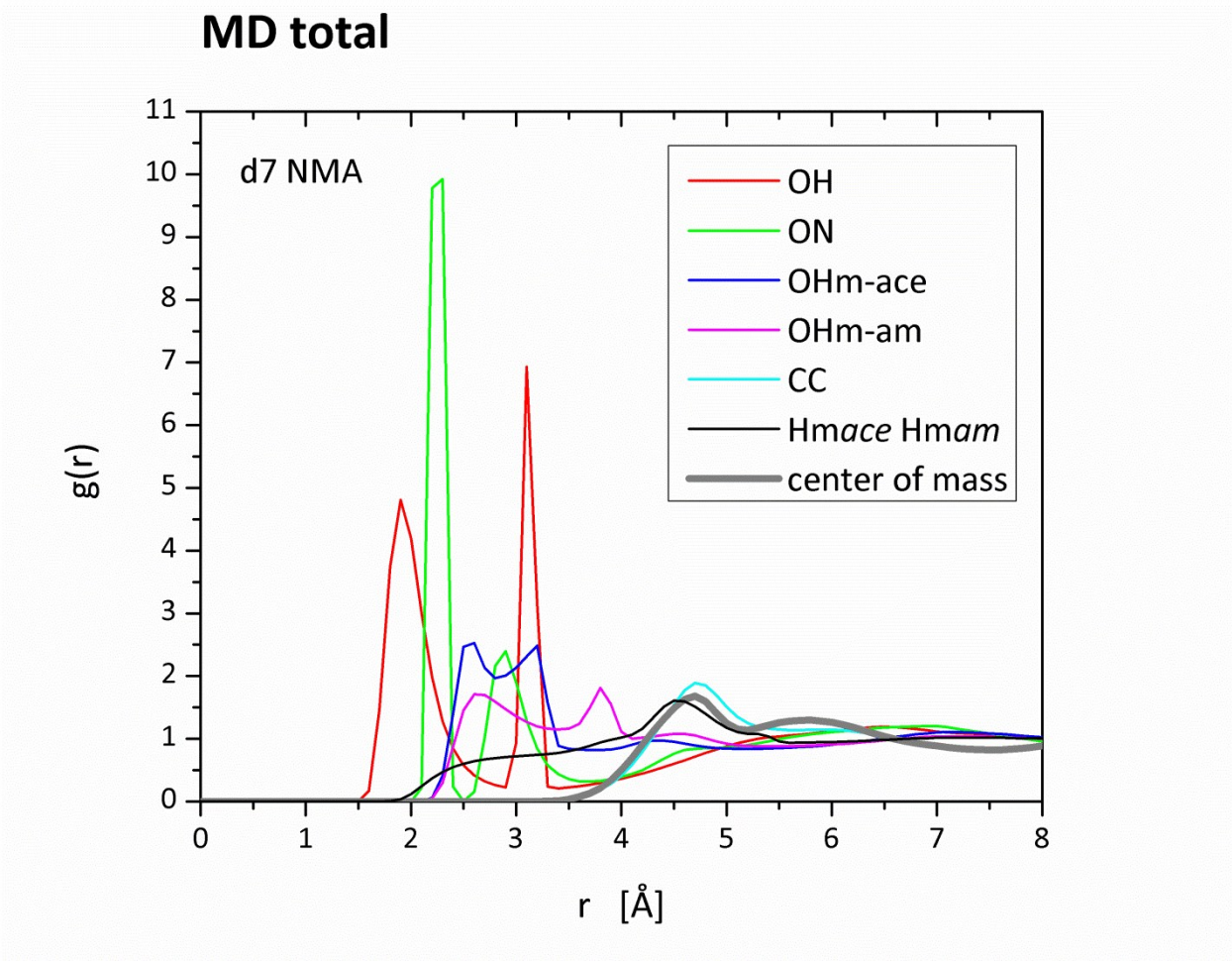


**Figure S3.** Partial radial distribution functions of NMA, as shown in Figure 1b of the main text. Here the figure includes both intramolecular and intermolecular contributions. In the legend, OH refers to pair correlations between the carbonyl oxygen and the amine hydrogen, ON refers to those between the carbonyl oxygen and backbone nitrogen, OHm-ace refers to the correlations between the oxygen atom and the hydrogen atoms in the acetyl methyl group, while Ohm-am refers to the correlations between the oxygen atom and the amide methyl group. CC represents corellations between carbonyl carbon atoms. Hmace Mmam corresponds to correlations between the hydrogen atoms in the acetyl and amide methyl groups respectively. Center of mass the refers to correlations between molecular centers of mass. Note the strong contributions of some intramolecular features.

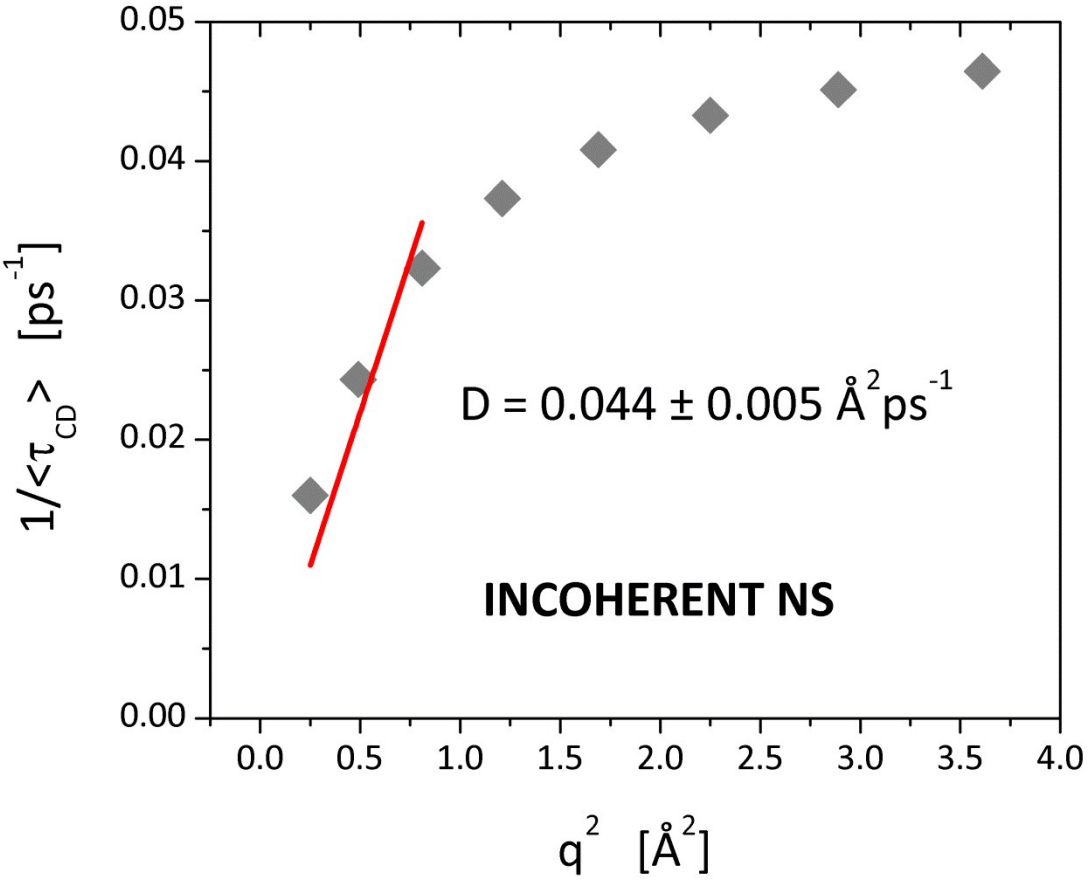


**Figure S4** Estimate of NMA self-diffusion coefficient from extrapolation at lowest three q-values where the presence of the 'cage' is less prevalent. The value of 0.044 $Å^2ps^{-1}$ is n reasonable agreement with the estimate from MD and prior literature.

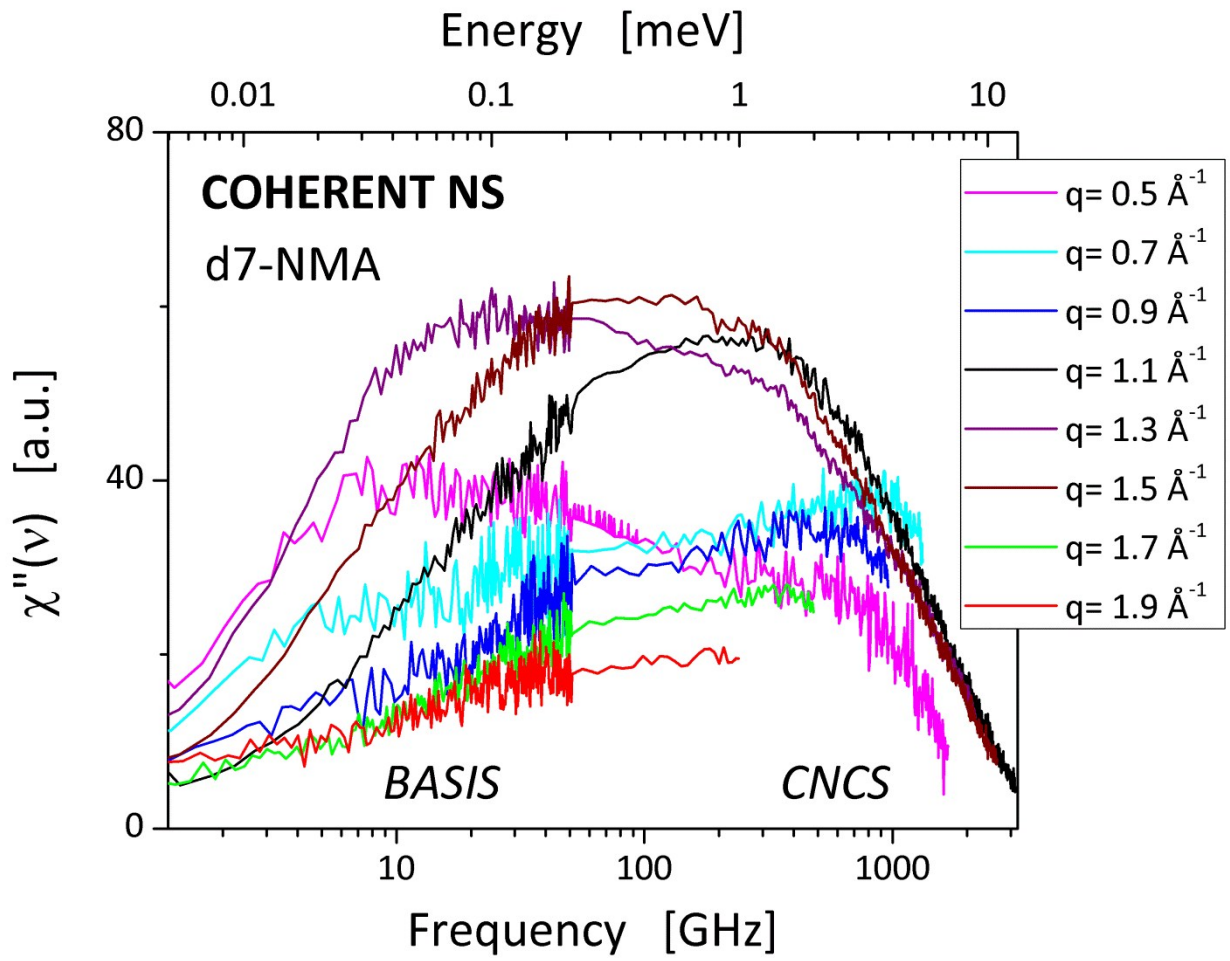


**Figure S5** Coherent NS spectra following removal of the incoherent contribution in completion of Figure 4c of the main text.

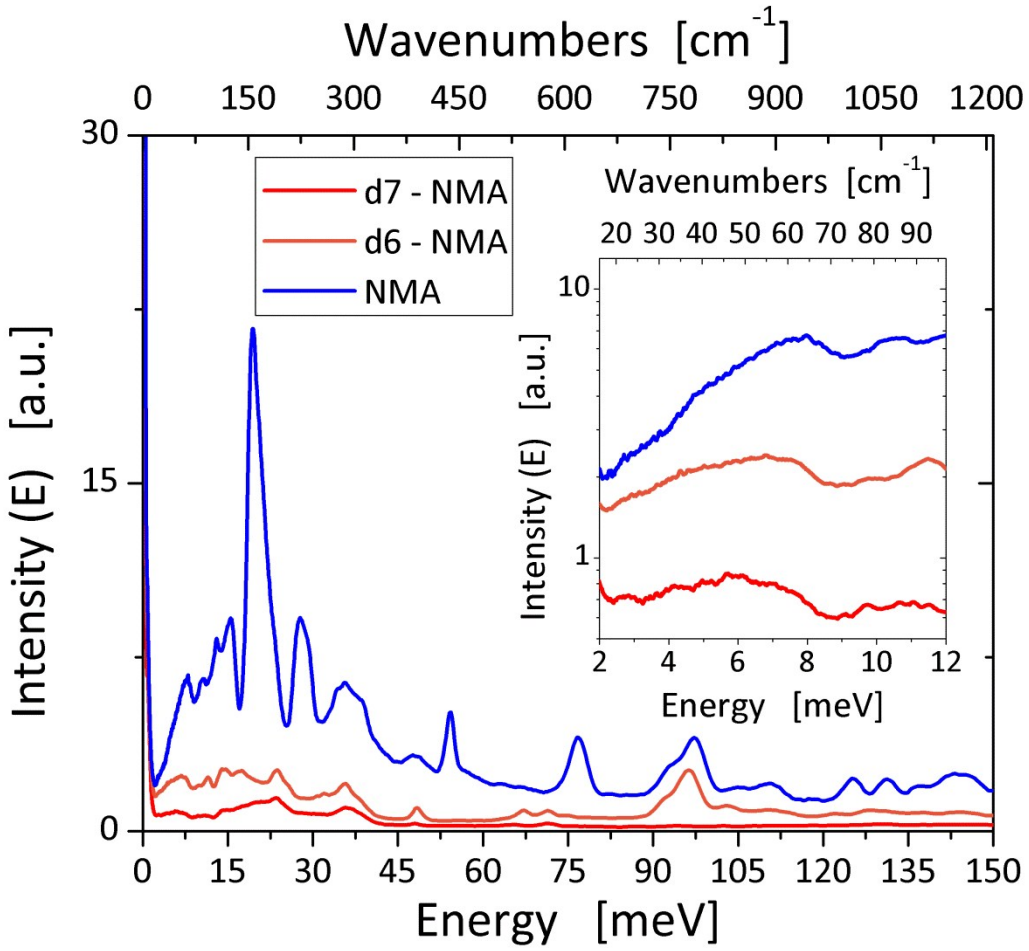


**Figure S6** Vibrational spectra collected on VISION spectrometer on NMA isotopes at 10K, inset demonstrates the differences in vibrational spectra between the isotopic variants.

**REFERENCES**


1. Neuefeind, J.; Feygenson, M.; Carruth, J.; Hoffmann, R.; Chipley, K. K. *Nuclear Instruments and Methods in Physics Research Section B: Beam Interactions with Materials and Atoms* **2012,** 287, (0), 68-75.
2. Mamontov, E.; Herwig, K. W. *Review of Scientific Instruments* **2011,** 82, (8), 085109.
3. Ehlers, G.; Podlesnyak, A. A.; Niedziela, J. L.; Iverson, E. B.; Sokol, P. E. *Review of Scientific Instruments* **2011,** 82, (8), 085108.
4. Berchiesi, G.; Vitali, G.; Amico, A. *Journal of molecular liquids* **1986,** 32, (2), 99-109.
5. Bée, M. *Adam Hilger, Bristol, UK* **1988**.
6. Alvarez, F.; Alegra, A.; Colmenero, J. *Physical Review B* **1991,** 44, (14), 7306.
7. Lindsey, C.; Patterson, G. *The Journal of chemical physics* **1980,** 73, (7), 3348-3357.
8. Hunt, N. T.; Turner, A. R.; Tanaka, H.; Wynne, K. *The Journal of Physical Chemistry B* **2007,** 111, (32), 9634-9643.
9. Arbe, A.; Colmenero, J.; Alvarez, F.; Monkenbusch, M.; Richter, D.; Farago, B.; Frick, B. *Physical Review E* **2003,** 67, (5), 051802.
10. Chen, L.; Gross, T.; Lüdemann, H.-D. *Zeitschrift für Physikalische Chemie International journal of research in physical chemistry and chemical physics* **2000,** 214, (2/2000), 239.
11. Pattanayak, S. K.; Prashar, N.; Chowdhuri, S. *The Journal of chemical physics* **2011,** 134, (15), 154506.
12. Seeger, P. A.; Daemen, L. L.; Larese, J. Z. *Nuclear Instruments and Methods in Physics Research Section A: Accelerators, Spectrometers, Detectors and Associated Equipment* **2009,** 604, (3), 719-728.
13. Darden, T.; York, D.; Pedersen, L. *The Journal of chemical physics* **1993,** 98, (12), 10089-10092.
14. Hess, B.; Bekker, H.; Berendsen, H. J.; Fraaije, J. G. *Journal of computational chemistry* **1997,** 18, (12), 1463-1472.
15. Guvench, O.; Mallajosyula, S. S.; Raman, E. P.; Hatcher, E.; Vanommeslaeghe, K.; Foster, T. J.; Jamison, F. W. *Journal of chemical theory and computation* **2011,** 7, (10), 3162.
16. Pronk, S.; Páll, S.; Schulz, R.; Larsson, P.; Bjelkmar, P.; Apostolov, R.; Shirts, M. R.; Smith, J. C.; Kasson, P. M.; van der Spoel, D. *Bioinformatics* **2013**, btt055.
17. Mazza, M. G.; Giovambattista, N.; Stanley, H. E.; Starr, F. W. *Physical Review E* **2007,** 76, (3), 031203.
18. Mazza, M. G.; Giovambattista, N.; Starr, F. W.; Stanley, H. E. *Physical review letters* **2006,** 96, (5), 057803.
19. Kob, W.; Donati, C.; Plimpton, S. J.; Poole, P. H.; Glotzer, S. C. *Physical review letters* **1997,** 79, (15), 2827.
20. Rahman, A. *Physical Review* **1964,** 136, (2A), A405.
21. van der Spoel, D.; van Maaren, P. J.; Larsson, P.; Tîmneanu, N. *The Journal of Physical Chemistry B* **2006,** 110, (9), 4393-4398.
22. Luzar, A. *The Journal of Chemical Physics* **2000,** 113, (23), 10663-10675.
23. Luzar, A.; Chandler, D. *Nature* **1996,** 379, (6560), 55.
24. Williams, G.; Watts, D. C. *Transactions of the Faraday Society* **1970,** 66, 80-85.
25. Williams, G.; Watts, D. C.; Dev, S.; North, A. *Transactions of the faraday Society* **1971,** 67, 1323-1335.
26. Eyring, H. *The Journal of chemical physics* **1936,** 4, (4), 283-291.